

0935

Quantification of exchange in the mouse brain using double diffusion encodings with fixed total diffusion-weighting

Teddy Xuke Cai^{1,2}, Nathan Hu Williamson^{2,3}, Peter Joel Basser², Mohamed Tachrount¹, and Karla Loreen Miller¹¹Wellcome Centre for Integrative Neuroimaging, FMRIB, Nuffield Department of Clinical Neurosciences, University of Oxford, Oxford, United Kingdom, ²Section on Quantitative Imaging and Tissue Sciences, Eunice Kennedy Shriver National Institute of Child Health and Human Development, NIH, Bethesda, MD, United States, ³National Institute of General Medical Sciences, NIH, Bethesda, MD, United States

Synopsis

Keywords: Diffusion Acquisition, Diffusion/other diffusion imaging techniques, Exchange

Motivation: Exchange is an important effect in diffusion MR of the brain but remains difficult to quantify using conventional methods and signal models due to parameter degeneracy.

Goal(s): To develop and demonstrate robust measurement of exchange in the mouse brain.

Approach: A method based on double diffusion encoding was previously developed to probe exchange isolated from other effects, yielding robust exchange time measurements. We apply this method *in vivo* for the first time.

Results: We report a fast *in vivo* exchange time of approximately 38 ms as compared to 146 ms in a fixed sample, obtained by averaging through a slice.

Impact: Cellular water exchange reflects not only structural characteristics but has also been linked to metabolism. Quantifying exchange may yield rich information, yet methods to do so are not mature. Here, we demonstrate a unique, isolated measurement of exchange *in vivo*.

Introduction

The exchange of water between biological microenvironments, namely the intra- and extracellular space, is increasingly recognized as an important effect in diffusion MR of the brain.¹⁻³ Exchange has also recently been linked to steady-state, metabolic activity⁴⁻⁶, and may thus be a valuable biomarker. Despite growing interest, a standard diffusion MR method to measure exchange has yet to emerge. Various methods have been proposed^{3,7-9} (e.g., NEXI¹⁰), but these generally do not isolate exchange – rather, exchange is modelled in tandem with microstructural parameters, resulting in issues of parameter degeneracy. The difficulty of incorporating exchange into compartment signal models may explain, in part, the wide range of reported exchange times τ_k in the literature, which span from $\tau_k \approx 3 - 500$ ms, even in similar tissue.^{1,3} These disparate reports indicate that the quantification of exchange remains an open problem.

Previous work based on diffusion exchange spectroscopy (DEXSY)¹¹ – a double diffusion encoding method – showed that with just two acquisitions per mixing time, one can separate exchange from other effects.¹²⁻¹⁵ Thus, this method overcomes the issue of parameter degeneracy, and τ_k can be quantified without simultaneously estimating parameters such as intra-/extracellular diffusivities. Here, we provide the first proof-of-concept demonstration of this method in mouse brain, *in vivo* and in a fixed sample, paving the way for future developments towards quantitative exchange imaging.

Theory

The method is based on sub-sampling the 3D parameter space of the DEXSY experiment, which consists of two diffusion encodings (b_1, b_2), separated by a longitudinal storage/mixing time, t_m . As previously shown^{12,14}, holding the sum of b-values constant – $b_s = b_1 + b_2$ – removes the effect of non-exchanging, Gaussian diffusion, leaving non-Gaussian diffusion and exchange.^{14,15} These effects can be captured in the log-ratio of two acquisitions: (i) with equal diffusion-weighting $b_1 = b_2 = b_s/2$, denoted $S_{b_1=b_2}$, and (ii) with $b_1 = b_s, b_2 = 0$, denoted $S_{b_1=b_s}$. The evolution of this log-ratio with t_m separates exchange from non-Gaussian diffusion, as non-Gaussian diffusion does not vary with t_m , but manifests in the intercept. Exchange can then be fit to a first-order model:

$$-\ln\left(\frac{S_{b_1=b_2}}{S_{b_1=b_s}}\right) = C_1 \exp\left(-\frac{t_m}{\tau_k}\right) + C_0,$$

where C_0 captures non-Gaussian diffusion, exchange during the encoding, and T_2 - T_2 exchange, and C_1 is proportional to the experimentally observable exchange. Taking a log-ratio also removes t_m -dependent effects, namely T_1 -relaxation.

Methods

A stimulated echo DEXSY sequence was implemented on a horizontal-bore 7-T Bruker BioSpec 70/20 (Ettlingen, Germany), using an 86 mm transmit RF coil and a 4-channel CryoProbe for the receive coil (Bruker, Germany). The sequence uses bipolar gradients to achieve double diffusion encoding with a chosen $b_s = 3500$ s/mm², varying the amplitude to acquire either $S_{b_1=b_2}$ or $S_{b_1=b_s}$ (Fig. 1). Gradients were oriented in the slice direction (rostral-caudal). A standard EPI readout was used for imaging (0.4 × 0.4 mm in-plane, 0.75 mm slice thickness). Additionally, $\delta/\Delta = 4.5/8$ ms, and TE = 21.6 ms. TR was variable with a recovery time of 3.6 or 7.2 s (NR = 10 or 5, using the median) in the fixed sample or *in vivo*, respectively. 18 mixing times were acquired from $t_m = 2 - 500$ ms, for a per-slice, per-repetition scan time of 4 min.

Animal procedures were approved by the local Animal Welfare and Ethical Review Body. A C57BL6J wild-type adult mouse (n = 1, male) was scanned.

Results

In Fig. 2, the raw *in vivo* images $S_{b_1=b_2}$ and $S_{b_1=b_s}$ at selected t_m are shown for an exemplar slice. The slice means after masking of the brain were analyzed (rather than individual voxels) due to SNR difficulties arising from the combination of images. In Fig. 3a, the slice means from Fig. 2 are plotted vs. t_m . While both means exhibit decay with t_m primarily due to T_1 -relaxation, $S_{b_1=b_2}$ exhibits additional decay attributable to exchange. The log-ratio was then fit to Eq. 1, shown in Fig. 3b, yielding $\tau_k \approx 38$ ms.

Analogous results are shown in Figs. 4 and 5 for a fixed sample, yielding $\tau_k \approx 146$ ms.

Discussion and Conclusions

The estimated $\tau_k \approx 38$ ms *in vivo* lies on the faster end of estimates in the literature^{1,3} and is of the same order-of-magnitude as previous results $\tau_k \approx 13$ ms obtained in viable, *ex vivo* neonatal mouse spinal cord^{6,13,15}, which is mostly gray matter. The longer τ_k here may result from averaging through a slice containing (less permeable) white matter. The even longer $\tau_k \approx 146$ ms in fixed tissue supports the hypothesis that exchange is linked to activity. Importantly, these results also suggest that exchange cannot be ignored in diffusion MR measurements with typical encoding times of $\Delta \sim 20 - 40$ ms.

The presented results, while preliminary, demonstrate the feasibility of an isolated exchange measurement. No microstructural parameters are estimated in Eq. 1, and the parameters C_0, C_1 correspond merely to an intercept and limit in the log-ratio. With further SNR developments, robust *in vivo* imaging of τ_k may be achieved using this method.

Acknowledgements

MT and KLM contributed equally to this work.

TXC and PJB were supported by the IRP of the NICHD.

NHW was funded by the NIGMS PRAT Fellowship Award #FI2GM133445-01.

The Wellcome Centre for Integrative Neuroimaging is supported by core funding from the Wellcome Trust (203139/Z/16/Z), which funds MT. KLM is supported by a Wellcome Trust Senior Research Fellowship (224573/Z/21/Z).

References

- Nilsson M, van Westen D, Ståhlberg F, Sundgren PC, Lätt J. The role of tissue microstructure and water exchange in biophysical modelling of diffusion in white matter. *MAGMA*. 2013;26(4):345-70.
- Jelescu IO, Palombo M, Bagnato F, Schilling KG. Challenges for biophysical modeling of microstructure. *Journal of Neuroscience Methods*. 2020;344:108861.
- Olesen JL, Østergaard L, Shemesh N, Jespersen SN. Diffusion time dependence, power-law scaling, and exchange in gray matter. *NeuroImage*. 2022;251:118976.
- Springer CS, Baker EM, Li X, et al. Metabolic activity diffusion imaging (MADI): I. Metabolic, cytometric modeling and simulations. *NMR in Biomedicine*. 2023;36(1): e4781.
- Springer CS, Baker EM, Li X, et al. Metabolic activity diffusion imaging (MADI): II. Noninvasive, high-resolution human brain mapping of sodium pump flux and cell metrics. *NMR in Biomedicine*. 2023;36(1):e4782.
- Williamson NH, Ravin R, Cai TX, Falgairolle M, O'Donovan MJ, Basser PJ. Water exchange rates measure active transport and homeostasis in neural tissue. *PNAS Nexus*. 2023;2(3):pgad056.
- Kärger J. NMR self-diffusion studies in heterogeneous systems. *Advances in Colloid and Interface Science*. 1985;23:129-48.
- Åslund I, Nowacka A, Nilsson M, Topgaard D. Filter-exchange PGSE NMR determination of cell membrane permeability. *Journal of Magnetic Resonance*. 2009;200(2):291-5.
- Chakwizira A, Westin C, Brabec J, et al. Diffusion MRI with pulsed and free gradient waveforms: Effects of restricted diffusion and exchange. *NMR in Biomedicine*. 2023;36(1):e4827.
- Jelescu IO, de Skowronski A, Geffroy F, Palombo M, Novikov DS. Neurite Exchange Imaging (NEXI): A minimal model of diffusion in gray matter with inter-compartment water exchange. *NeuroImage*. 2022;256:119277.
- Callaghan PT, Furó I. Diffusion-diffusion correlation and exchange as a signature for local order and dynamics. *The Journal of Chemical Physics*. 2004;120(8):4032-8.

12. Cai TX, Benjamini D, Komlos ME, Bassar PJ, Williamson NH. Rapid detection of the presence of diffusion exchange. *Journal of Magnetic Resonance*. 2018;297:17-22.
13. Williamson NH, Ravin R, Benjamini D, et al. Magnetic resonance measurements of cellular and sub-cellular membrane structures in live and fixed neural tissue. *eLife*. 2019;8:e51101.
14. Williamson NH, Ravin R, Cai TX, et al. Real-time measurement of diffusion exchange rate in biological tissue. *Journal of Magnetic Resonance*. 2020;317:106782.
15. Cai TX, Williamson NH, Ravin R, Bassar PJ. Disentangling the effects of restriction and exchange with diffusion exchange spectroscopy. *Frontiers in Physics*. 2022;10: 805793.

Figures

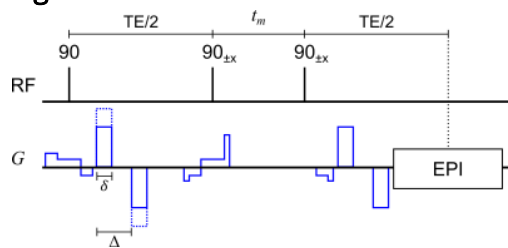


Figure 1. Stimulated echo DEXSY sequence with EPI readout. Bipolar gradients (blue) are implemented during each encoding in the same direction as slice selection (rostral-caudal) and are drawn roughly to scale with experimental parameters. Solid and dashed lines represent the $S_{b_1=b_2}$ and $S_{b_1=b_s}$ acquisitions, respectively. Spoilers and a two-step phase cycle of the storage pulses are also implemented.

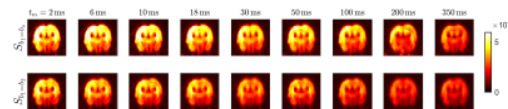


Figure 2. Raw DEXSY images $S_{b_1=b_2}$ and $S_{b_1=b_s}$ acquired *in vivo*. Images are shown for an exemplar slice and at selected values of t_m . Each voxel is from the median of 5 repetitions.

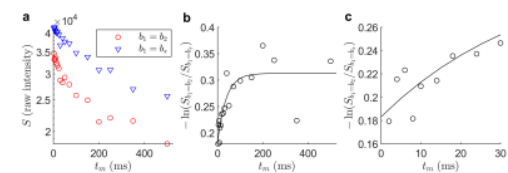


Figure 3. Fitting of exchange to the slice means from Fig. 2. (a) Slice means plotted vs. t_m . Note the additional decay of $S_{b_1=b_2}$ compared to $S_{b_1=b_s}$ over the initial range of t_m . (b) Fitting of the log-ratio to Eq. (1), which yields $\tau_k \approx 38$ ms. The intercept parameter $C_0 \approx 0.18$ captures the extraneous effects of non-Gaussian diffusion, exchange during the encoding and TE, and T_2 - T_2 exchange. (c) Same plot as in (b) zoomed in on the initial rise up to $t_m = 30$ ms.

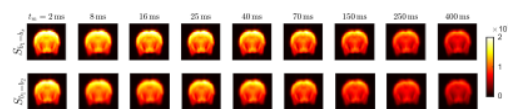


Figure 4. Raw DEXSY images $S_{b_1=b_2}$ and $S_{b_1=b_s}$ in a fixed sample for an exemplar slice at selected values of t_m . Each voxel is from the median of 10 repetitions.

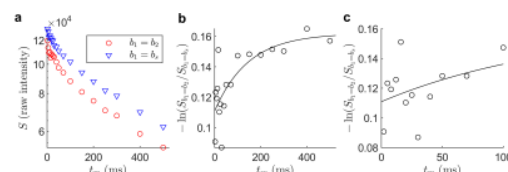


Figure 5. Fitting of exchange to the slice means from Fig. 4. (a) Slice means plotted vs. t_m . (b) Fitting the log-ratio to Eq. (1), yielding $\tau_k \approx 146$ ms. (c) Same plot as in (b) zoomed in on the initial rise up to $t_m = 100$ ms.